SLAC-PUB-782
(TH)
August 1970

FIELD THEORY REALIZATION OF THE DROPLET MODEL*

Shau-Jin Chang

Physics Department
University of Illinois,† Urbana, Illinois 61801

and

Stanford Linear Accelerator Center
Stanford University, Stanford, California 94305

(Submitted to The Physical Review)

*Work supported in part by the U. S. Atomic Energy Commission and the National Science Foundation under Contract No. NSF GP 19433.

†Permanent address.

ABSTRACT

We demonstrate with two field-theoretic models that the operator droplet model proposed by Chou and Yang can be understood as due to the contribution from a class of leading Feynman diagrams at $s = \infty$. In the first model, we consider a theory which consists of both a strong and an EM interaction. The purpose of introducing two types of interactions is to supply a natural division between the production of particles and the interaction between the jets. In this model, the sum of pure photon exchange diagrams leads automatically to an expression identical to that of the operator droplet model. Limitations and generalizations of the model are investigated. The second model is derived from pure quantum electrodynamics. We find that an operator droplet model formulation can reproduce leading amplitudes in quantum electrodynamics, including those which give rise to $(\ell n s)^N$ behavior. This confirms and generalizes an earlier result of Lee. We demonstrate explicitly how the N-bubble diagrams should be treated in this calculation. By including diagrams related to one another by covariance, a reference-frame-independent result always emerges. These frame-independent results coincide with earlier calculations based on the usual Feynman rules.

1. INTRODUCTION

Chou, Yang[1] and their coworkers have proposed that the high energy scattering can be understood qualitatively by a droplet model. In particular, they conjectured that hadron production processes can be understood through an operator version of the droplet model. In a recent article,[2] the operator droplet model was put into an elegant and useful form by Lee. Lee then applied the operator droplet model to quantum electrodynamics (QED), with the identification of the matter density ρ and the charge density. He demonstrated that this model can reproduce the field-theoretic results of Cheng and Wu[3] as to impact factors. It is interesting to know whether or how more complicated $(\ell ns)^N$-dependent terms can be obtained in Lee's formulation. It is also important to find out if his conclusion can be generalized to high order processes.

The purpose of this paper is to show that the operator droplet model results can indeed be obtained by summing proper set of diagrams. By establishing the connection between a physical model and a category of Feynman diagrams, one can hope to gain some insights and understanding of the model, such as its possible limitations and generalizations. This is one of the important reasons for carrying out a systematical analysis of Feynman diagrams.

The first model that we shall study is a combination of a pseudoscalar meson theory and the electromagnetic (EM) interaction. We first analyze a diagram by decomposing it into units which are joined together by pure photon exchange.[4] Each of these units defines a primitive piece, as introduced in paper III. For simplicity, we shall ignore further EM interactions within these primitive units (hereafter referred as hadronic blobs). In this way, we make a division between the hadronic interactions within the blobs and the EM interactions between the blobs. The dynamical distinction of these two interactions is important in

the first model to achieve our conclusion. An especially simple set of diagrams according to this classification is shown in Fig. 1, in which there is no further hadronic bubbles lying between the blobs associated with the incident particles. By summing over diagrams of this category, we obtain a result which can be identified with that of an operator droplet model with an s-independent potential. This potential is the two-dimensional Fourier transform of the one-photon propagator. Contributions due to further photon-photon interactions can be partially handled if one modifies the potential to include all connected diagrams. The modified potential acquires an s-dependence.

In pure QED calculations, the sum of diagrams in Fig. 1 no longer exponentiates to a droplet model form. However, the operator droplet model can be recovered formally if one includes <u>all</u> leading graphs and if proper care is taken in defining the infinite momentum matrix element of the product of currents. Formal perturbative calculation reveals that for a certain important class of final and intermediate states, the matrix element of the currents diverges logarithmically at large s. This indicates that there is some implicit s-dependences in the QED expression described by the operator droplet model. This implicit s-dependence is associated with the increase of the available $\ell n\, p_+$ phase space at $s \to \infty$.[5] Once we realize the origin of this hidden ℓn s-dependence, we can reproduce all the leading amplitudes in QED from an operator droplet model expression suggested by Chou and Yang,[1] and by Lee.[2]

The paper is organized as follows. In Section 2, we consider a model in which a strong interaction and the EM interaction are treated separately. We analyze a particular category of diagrams due to multiphoton exchange and show that it leads naturally to an expression identical to the operator droplet model. A simpler and more straightforward derivation is obtained in Section 3, based

on essentially the same assumptions. In Section 4, a generalization of this model to include a larger set of diagrams is outlined. In Section 5, we demonstrate how the operator droplet model can be used to compute leading QED diagrams, including those which give rise to $(\ell n\, s)^N$ behavior at large s. The conclusion and a comparison of our model to Feynman's parton model[6,7] comprise the contents of the last section. We also include a short appendix to demonstrate how one can obtain commutator relations on the light cone from the conventional equal-time commutator relations.

2. MULTIPHOTON EXCHANGE DIAGRAMS

We consider a simple field theory model with both a strong and an EM interaction, $\mathscr{L}_{int} = \mathscr{L}_s + \mathscr{L}_{EM}$. We may take the strong interaction, for example, as pseudoscalar mesons $\underset{\sim}{\phi}$ coupled to nucleons ψ through the coupling $\mathscr{L}_s = ig\, \bar{\psi}\, i\gamma_5 \frac{\tau}{2}\, \psi\, \underset{\sim}{\phi}$, or as quark-quark interactions. The conclusions of this paper do not depend on the detailed structure of the strong interaction as long as there is no <u>fundamental</u> strongly interacting vector field. The EM interaction, on the other hand, is mediated by a vector field (the Maxwell field) $\mathscr{L}_{EM} = ej_\mu A^\mu$ with

$$j_\mu = \bar{\psi}\, \gamma_\mu \psi \quad . \tag{2.1}$$

To avoid infrared divergences, we give our photon a fictitious mass μ. Note that our results are readily applicable to pure hadronic processes if one replaces the photon by a vector meson, or a flat Pomeron. We call our vector meson a "photon" solely for simplicity.

In paper II, we demonstrated that those diagrams whose contribution remains large at large s but fixed t are the diagrams which can be separated into two fast moving parts joining together by vector mesons (here photons) only.

Some typical diagrams of this category are shown in Fig. 1. Figure 1 describes the amplitude due to pure photon exchange without further interactions among the exchanged photons. The blobs appearing here are primitive pieces, i.e., they can not be separated into two or more parts by cutting photon lines only, as demonstrated in Fig. 1. We now consider a subclass of diagrams in Fig. 1 in which we also ignore the EM interactions (radiative correction, etc.) within the hadronic blobs. As we shall see, summing over diagrams of this latter type leads to expressions identical to the operator droplet model conjectured by Chou and Yang.[1]

The purpose of introducing two types of interaction here is to provide a clear cut separation between the mechanism for production of final particles and the interaction between the jets. As we shall see in more detail in Section 4, this kind of distinction is not possible for pure QED calculations.

In III, we showed that the amplitude for diagram 1 can be written, in the limit of large s, as

$$M = \frac{s}{2}\int \Pi \frac{dq'_-}{4\pi} A_{++\ldots+}(p'_a, q') \; 4\pi \; \delta(\Sigma q'_- - k'_-)$$

$$\Pi \frac{dq''_+}{4\pi} \; C_{--\ldots-}(p''_c, q'') \; 4\pi \; \delta(\Sigma q''_+ - k''_+) \qquad (2.2)$$

$$\Pi\left(\frac{d^2 q_i}{(2\pi)^2} \; \frac{-ie^2}{q_i^2 + \mu^2}\right) \; (2\pi)^2 \; \delta^2(\Sigma \underset{\sim}{q}_i - \underset{\sim}{k}) \quad ,$$

where k is the momentum transfer. $A_{\mu\nu\ldots\sigma}(p', q')$ is the partial amplitude for the LHS of graph 1, evaluated in the standard frame (essentially the lab frame)

of particle a, defined by

$$
\begin{aligned}
&p'_{a+} \equiv p'^{0}_{a} + p'^{3}_{a} = 1, \\
&p'_{ai+} \equiv p_{ai+}/p_{a+} \quad , \qquad 0 < p'_{ai+} < 1 \, , \\
&\underset{\sim}{p}'_{ai} \equiv \underset{\sim}{p}_{ai} \quad , \\
&p'_{ai-} \equiv p'^{0}_{ai} - p'^{3}_{ai} \equiv (p_{a+})\, p_{ai-} \quad .
\end{aligned}
\tag{2.3}
$$

The plus and minus appearing in (2.2) represent the four-vector indices 0+3 and 0-3. The variables p'_+, $\underset{\sim}{p}'$, the fractional longitudinal momentum and the transverse momentum, form a very convenient parameterization for describing high energy scattering. Readers are invited to consult II and III for more detailed kinematics of this infinite momentum frame.

Similarly, $C_{\mu\nu\ldots\sigma}(p'',q')$ is the partial amplitude of the RHS of graph 1, evaluated in the standard frame of particle c:

$$
\begin{aligned}
&p''_{c-} \equiv p''^{0}_{c} - p''^{3}_{c} = 1 \quad , \\
&p''_{ci-} \equiv p_{ci-}/p_{c-} \quad , \qquad 0 < p''_{ci-} < 1 \\
&\underset{\sim}{p}''_{ci} \equiv \underset{\sim}{p}_{ci} \quad , \qquad \underset{\sim}{p}''_{ci+} \equiv (p_{c-})\, p_{ci+}
\end{aligned}
\tag{2.4}
$$

The momentum variables for the exchange photon can be chosen as q''_+, $\underset{\sim}{q}' = \underset{\sim}{q}''$, and q'_-. The other combinations $q'_+ = q''_+/s$, $q''_- = q'_-/s$ vanish at $s = \infty$.

The amplitude $A_{\mu\nu\ldots\sigma}(p_a, q)$ is a generalized vertex function. First, we wish to point out that the above amplitude is related to the matrix element of the

Heisenberg operators j_μ for the strong interaction alone through

$$\int \prod_j d^4x_j \, e^{-i\sum q_i\cdot x_i} \langle A|T\left(j_\mu(x_1) \cdots j_\lambda(x_N)\right)|a\rangle \tag{2.5}$$

$$= (2\pi)^4 \delta^4(p_a+q-\sum p_{ai}) \times \sum_{\substack{\text{all possible}\\ \text{N-photon subgraph}}} A_{\mu\nu\ldots\lambda}(p_a,q)$$

where $q=\sum q_j$, a, A are shorthand notations for initial particle a and its products A. We shall sometimes refer to A as jet A.[8] After including all N-photon exchange diagrams, we also find that Eq. (2.2) reduces to

$$M^{(N)} = \frac{s}{2} \sum_{\substack{\text{all possible}\\ \text{N-photon diagram}}} \int \prod \frac{dq'_-}{4\pi} \cdot A_{++\ldots+}(p'_a,q') \, 4\pi\,\delta(\textstyle\sum q'_- - k'_-)$$

$$\prod \frac{dq''_+}{4\pi} \cdot C_{--\ldots-}(p''_c,q'') \, 4\pi\,\delta(q''_+ - k''_+)$$

$$\times \prod \frac{d^2q_i}{(2\pi)^2} \frac{-ie^2}{q_i^2+\mu^2} (2\pi)^2 \delta^2(\textstyle\sum \underset{\sim}{q}_i - \underset{\sim}{k})$$

$$= \frac{s}{2} \frac{1}{N!} \int \prod \frac{dq'_-}{4\pi} \left[\sum_{\substack{\text{all sub-}\\ \text{graph}}} A_{++\ldots+}(p'_a,q')\right] 4\pi\,\delta(\textstyle\sum q'_- - k'_-)$$

$$\prod \frac{dq''_+}{4\pi} \cdot \left[\sum_{\substack{\text{all sub-}\\ \text{graph}}} C_{--\ldots-}(p''_b,q'')\right] 4\pi\,\delta(\textstyle\sum q''_+ - k''_+)$$

$$\times \prod \frac{d^2q_i}{(2\pi)^2} \frac{-ie^2}{q_i^2+\mu^2} (2\pi)^2 \delta^2(\textstyle\sum \underset{\sim}{q}_i - \underset{\sim}{k}) \quad . \tag{2.6}$$

By including all possible subgraphs in both A and C, we actually count diagrams with exchange photons labelled differently as different diagrams. The factor 1/N! is included to compensate the overcounting.

Now, the contribution for the subgraph A can be reduced to

$$(2\pi)^4\,\delta^4(p'_a+k'-\Sigma\,p'_{ai})\int\Pi\,\frac{dq'_-}{4\pi}\sum_{\substack{\text{all sub-}\\ \text{graph}}} A_{++\ldots+}(p'_a,q')\Big|_{q'_+=0}\quad 4\pi\,\delta(\Sigma\,q'_--k'_-)$$

$$=\int\prod_j d^4x_j\int_{\text{loop}}\frac{dq'_-}{4\pi}\,e^{-i\sum_i q'_i x'_i}\,\langle A'|T\left(j_+(x'_1)\ldots j_+(x'_N)\right)|a'\rangle \qquad (2.7)$$

where A' and a' label jet A and particle a in the standard frame. By the use of

$$q'x'|_{q'_+=0}\;=\frac{1}{2}\,q'_-x'_+-\underset{\sim}{q}'\cdot\underset{\sim}{x}'\quad,$$

it is easy to carry out the q'_- (loop) integrals, giving

$$\prod_{\text{loop}}\int\frac{dq'_-}{4\pi}\,e^{-i\sum_i q'_i x'_i}\Big|_{q'_+=0}=\int dx'_+\;e^{i\underset{\sim}{q}_i\cdot\underset{\sim}{x}_i-\frac{i}{2}k'_-x'_+}\prod_i\,\delta(x'_{i+}-x'_+)\quad. \qquad (2.8)$$

The δ-functions in (2.8) insure that the $j_+(x'_i)$ appearing in (2.7) are at equal x_+. It is shown in the Appendix that the plus components of the EM current commute among themselves on the light cone x_+ = constant. Hence the T-product in (2.7) is the same as an ordinary product. This is important because we can now carry out the remaining integrals without worrying about the T-ordering:

$$\text{LHS of (2.7)} = 4\pi\;\delta(p'_{a-}+k'_- - \Sigma\,p'_{ai-})$$

$$\times\,\langle A'|\sigma_+(\underset{\sim}{q}_1)\;\ldots\;\sigma_+(\underset{\sim}{q}_N)\,|a'\rangle \qquad (2.9)$$

where

$$\sigma_+(\underset{\sim}{x}) = \frac{1}{2}\int dx_-\, j_+(x_+=0,\ \underset{\sim}{x},\ x_-) \quad , \tag{2.10}$$

$$\sigma_+(\underset{\sim}{q}) = \int d^2x\, e^{i\underset{\sim}{q}\cdot\underset{\sim}{x}}\, \sigma_+(\underset{\sim}{x}) \quad . \tag{2.11}$$

The operator $\sigma_+(\underset{\sim}{x})$ is essentially the $\sigma(\underset{\sim}{x})$ introduced by Lee.[2] It obeys the simple relations

$$\left[\sigma_+(\underset{\sim}{x}_1)\ ,\quad \sigma_+(\underset{\sim}{x}_2)\right] = 0 \quad ,$$

$$\int d^2x\, \sigma_+(\underset{\sim}{x}) = Q \ \text{(the charge operator)} \quad ,$$

and the T.C.P. transformation properties as demonstrated by Lee.

An analogous result holds for the partial amplitude $C_{--\ldots-}(p_c'', q'')$,

$$(2\pi)^4\ \delta^4(p_c''-k''-\textstyle\sum p_{ci}'')\displaystyle\int \Pi\ \frac{dq_+''}{4\pi}\ C_{--\ldots-}(p_c'', q'')\Big|_{q_-''=0}\ 4\pi\ \delta(\textstyle\sum q_+''-k_+)$$

$$= 4\pi\ \delta(p_{c+}''-k_+''-\textstyle\sum p_{ci+}'')\times\left\langle C''\middle|\sigma_-(-\underset{\sim}{q}_1)\ldots\sigma_-(-\underset{\sim}{q}_N)\middle|\, c''\right\rangle \ , \tag{2.12}$$

with

$$\sigma_-(\underset{\sim}{y}) = \frac{1}{2}\int dy_+\, j_-(y_+,\ \underset{\sim}{y},\ y_-=0) \tag{2.13}$$

$$\sigma_-(\underset{\sim}{q}) = \int d^2y\ e^{i\underset{\sim}{q}\cdot\underset{\sim}{y}}\, \sigma_-(\underset{\sim}{y}) \quad . \tag{2.14}$$

c and C represent particle c and its products (jet C). The double prime on a symbol indicates that the quantity is measured in the standard frame of particle

c. Putting Eqs. (2.9) - (2.14) together and performing k integrals, we find

$$M^{(N)}(2\pi)^4\,\delta(p'_{a+}-\Sigma p'_{ai+})\,\delta(p''_{c-}-\Sigma p''_{ci-})\,\delta^2(\underset{\sim}{p}_a+\underset{\sim}{p}_c-\Sigma\underset{\sim}{p}_{ai}-\Sigma\underset{\sim}{p}_{ci})$$

$$=\frac{s}{2}\,\frac{1}{N!}\int\Pi\frac{d^2q_i}{(2\pi)^2}\,\frac{-ie^2}{\underset{\sim}{q}_i^2+\mu^2}\times$$

$$\times\langle A'|\sigma_+(\underset{\sim}{q}_1)\cdots\sigma_+(\underset{\sim}{q}_N)|a'\rangle$$

$$\times\langle C''|\sigma_-(-\underset{\sim}{q}_1)\cdots\sigma_-(-\underset{\sim}{q}_N)|c''\rangle$$

$$=\frac{s}{2}\,\frac{1}{N!}\left\langle A',C''\left|\left[\int\frac{d^2q}{(2\pi)^2}\,\sigma_+(\underset{\sim}{q})\,\frac{-ie^2}{\underset{\sim}{q}^2+\mu^2}\,\sigma_-(\underset{\sim}{q})\right]^N\right|a',c''\right\rangle. \qquad (2.15)$$

In the last expression, it is understood that the operator σ_+ (σ_-) has only matrix element between the states associated with particle a (or particle c). The state $a',c'' = a' \times |c''\rangle$ is a shorthand notation for a state with particle a, c in their respective standard frames.

The total amplitude of Fig. 1, can be obtained from $M^{(N)}$ by summing over all N, giving

$$M(2\pi)^4\,\delta(p'_{a+}-\Sigma p'_{ai+})\,\delta(p''_{c-}-\Sigma p''_{ci-})\,\delta^2(\underset{\sim}{p}_a+\underset{\sim}{p}_c-\Sigma\underset{\sim}{p}_{ai}-\Sigma\underset{\sim}{p}_{ci})$$

$$=\frac{s}{2}\left\langle A',C''\left|\exp\left[\int\frac{d^2q}{(2\pi)^2}\,\sigma_+(\underset{\sim}{q})\,\frac{-ie^2}{\underset{\sim}{q}^2+\mu^2}\,\sigma_-(-\underset{\sim}{q})\right]-1\right|a',c''\right\rangle \qquad (2.16)$$

$$=\frac{s}{2}\left\langle A',C''\left|\exp\left[-ie^2\int d^2x\,d^2y\,\sigma_+(\underset{\sim}{x})\,V(\underset{\sim}{x}-\underset{\sim}{y})\,\sigma_-(\underset{\sim}{y})\right]-1\right|a',c''\right\rangle$$

with

$$V(\underset{\sim}{x})=\int\frac{d^2q}{(2\pi)^2}\,e^{i\underset{\sim}{q}\cdot\underset{\sim}{x}}\,\frac{1}{\underset{\sim}{q}^2+\mu^2} \qquad (2.17)$$

The exponentiation of a convolution of two operator densities is precisely the structure of the operator droplet model.

To obtain the original form of the model,[1] we follow the procedure developed by Lee. Introducing

$$2\pi\ \delta(p_{f+}-p_{i+})\ \langle\sigma_+(\underset{\sim}{x}_1+\underset{\sim}{z})\cdots\sigma_+(\underset{\sim}{x}_N+\underset{\sim}{z})\rangle_{fi}$$

$$\equiv\int\frac{d^2k}{(2\pi)^2}\ e^{-i\underset{\sim}{k}\cdot\underset{\sim}{z}}\langle p_f,\ \underset{\sim}{k}/2\,|\,\sigma_+(\underset{\sim}{x}_1)\cdots\sigma_+(\underset{\sim}{x}_N)\,|\,p_i,-\underset{\sim}{k}/2\rangle\ ,$$

$$\langle p_f,\ \underset{\sim}{k}/2\,|\,\sigma_+(\underset{\sim}{x}_1)\cdots\sigma_+(\underset{\sim}{x}_N)\,|\,p_i,\ -\underset{\sim}{k}/2\rangle$$

$$=2\pi\ \delta(p_{f+}-p_{i+})\int d^2z\ e^{i\underset{\sim}{k}\cdot\underset{\sim}{z}}\langle\sigma_+(\underset{\sim}{x}_1+\underset{\sim}{z})\cdots\sigma_+(\underset{\sim}{x}_N+\underset{\sim}{z})\rangle_{fi} \tag{2.18}$$

and analogous equations for σ_-'s, we have

$$M(2\pi)^4\,\delta(p'_{a+}-\Sigma p'_{ai+})\,\delta(p''_{c-}-\Sigma p''_{ci-})\,\delta^2(\underset{\sim}{p}_a+\underset{\sim}{p}_c-\Sigma\underset{\sim}{p}_{ai}-\Sigma\underset{\sim}{p}_{ci})$$

$$=\frac{s}{2}(2\pi)^2\,\delta(p'_{a+}-\Sigma p'_{ai+})\,\delta(p''_{c-}-\Sigma p''_{ci-})$$

$$\times\int dz\,dz'\,e^{i\underset{\sim}{k}\cdot\underset{\sim}{z}-i\underset{\sim}{k}'\underset{\sim}{z}'} \tag{2.19}$$

$$\times\left\langle\exp\left[-ie^2\int d^2x\,d^2y\ \sigma_+(\underset{\sim}{x}+\underset{\sim}{z})\ V(\underset{\sim}{x}-\underset{\sim}{y})\ \sigma_-(\underset{\sim}{y}+\underset{\sim}{z}')\right]-1\right\rangle_{A',C'';a',c'}.$$

After making the translations $\underset{\sim}{x}+\underset{\sim}{z}\to x$, $\underset{\sim}{y}+\underset{\sim}{z}'\to y$, and carrying out one z-integral for fixed $\underset{\sim}{b}=\underset{\sim}{z}'-\underset{\sim}{z}$, we have

$$M_{A',C'';a',c'}(k)=\frac{s}{2}\int d^2b\ e^{-i\underset{\sim}{k}\cdot\underset{\sim}{b}}\langle S(\underset{\sim}{b})-1\rangle_{A',C'';a',c'} \tag{2.20}$$

with

$$S(\underset{\sim}{b}) = \exp\left[-ie^2 \int \sigma_+(\underset{\sim}{x})\, V(\underset{\sim}{x}-\underset{\sim}{y}+\underset{\sim}{b})\, \sigma_-(\underset{\sim}{y})\, d^2x\, d^2y\right] \qquad (2.21)$$

Equation (2.20) is exactly the operator droplet model as conjectured by Chou and Yang.

3. AN ALTERNATIVE DERIVATION

We have found that the asymptotic amplitude due to set of diagrams 1 can be cast into a form suggested by the operator droplet model. Since the final answer is very simple, one expects that this result might be obtained more directly. Let us summarize the ingredients which enter into the derivation:

1. The scattering amplitude factors into two parts, one associated with the target and one associated with the projectile. The large component of the momentum in each part (p_+ for particle a and its products and p_- for particle c and its products) is preserved during the scattering. These two parts are joined together by vector mesons only.

2. The leading contribution of these diagrams comes from the plus components of the left-hand graph coupled with the minus components of the right-hand graph.

3. The proper variables to use in describing the amplitudes are those measured in the frames moving with the particles. These are standard frame variables for particle a and for particle c.

To give a simple derivation, we decompose the Hamiltonian into $H_0' + H_1'$ where H_0' consists of all kinematical terms as well as the strong interactions, and $H_1' = -\mathscr{L}_2' = e j^\mu A_\mu$ contains only the EM interaction. The s-matrix, in an interaction representation, is given by Dyson's equation,

$$S = T \exp\left(-ie \int d^4x\, j^\mu A_\mu\right) \qquad (3.1)$$

The effective s-matrix corresponding to Fig. 1 can be obtained from Eq. (3.1) by contracting out the Maxwell fields in the exponent, giving

$$S^{(\text{Fig. 1})} = T \exp\left[ie^2 \int dx\, dy\, j_\mu^{(a)}(x)\, D_F(x-y)\, j_\mu^{(c)}(y)\right] \tag{3.2}$$

Here $j_\mu^{(a)}$ represents the EM current interacting with particle a and jet A, $j_\mu^{(c)}$ represents the EM current interacting with particle c and jet C. Remember that we have included strong interactions exactly within the hadronic blobs for jet A and jet C. For the particular set of diagrams studied here, the strong interactions among jet A and jet C do not mix. Hence, we can treat them separately.

In the Heisenberg representation for the strong interaction alone, the matrix element for the diagrams of Fig. 1 is

$$\langle A, C\, T \exp\, -ie^2 \int d^4x\, d^4y\, j_\mu^{(a)}(x)\, D_F(x-y)\, j_\mu^{(c)}(y)\rceil\, |a,c\rangle\,. \tag{3.3}$$

Final states A, C describe the jets produced from the incident particles a and c respectively. Even though Eq. (3.3) is very similar in appearance to (2.16), these equations are in fact quite different. First, Eq. (3.3) contains a T-product. Second, the s-dependence of the amplitude is still implicit in (3.3).

To manifest the explicit behavior of the amplitude at $s \to \infty$, we make a Lorentz transformation for particle a and jet A from the c.m. frame to the standard frame of particle a:

$$\begin{aligned} |a\rangle &= U_a^{-1} |a'\rangle\,, \\ \langle A| &= \langle A'| U_a\,, \end{aligned} \tag{3.4}$$

$$U_a j^{(a)\mu}(x)\, U_a^{-1} = \begin{cases} \sqrt{s}\, j_+^{(a)}(x')\,, & \mu = + \\ j^{(a)}(x') & \perp \\ \dfrac{1}{\sqrt{s}}\, j_-^{(a)}(x')\,, & - \end{cases} \tag{3.5}$$

with

$$p'_{a+} = \frac{1}{\sqrt{s}} p_{a+} = 1, \quad \underset{\sim}{p}'_a = \underset{\sim}{p}_a, \quad p'_{a-} = \sqrt{s}\, p_{a-} \ ,$$
$$x'_+ = \frac{1}{\sqrt{s}} x_+ \ , \quad \underset{\sim}{x}' = \underset{\sim}{x}, \quad x'_- = \sqrt{s}\, x_- \ . \tag{3.6}$$

The momentum p and coordinate x are c.m. variables, as before. For simplicity, we assume that the states are normalized covariantly so that no additional kinematical terms arise during the Lorentz transformation. Similarly, we make a Lorentz transformation on particle c and jet C from the c.m. frame to standard frame c:

$$|c\rangle = U_c^{-1} |c''\rangle \ , \quad \langle C| = \langle C''| U_c \ ,$$
$$U_c\, j^{(c)\mu}\, U_c^{-1} = \begin{cases} \frac{1}{\sqrt{s}}\, j_+^{(c)}(y'') \\ \underset{\sim}{j}^{(c)}(y'') \\ \sqrt{s}\ j_-^{(c)}(y'') \end{cases} \tag{3.7}$$

with

$$p''_{c+} = \sqrt{s}\ p_{c+} \ , \quad \underset{\sim}{p}''_c = \underset{\sim}{p}_c \ , \quad p''_{c-} = \frac{1}{\sqrt{s}} p_{c-} = 1 \ ,$$
$$y''_+ = \sqrt{s}\ y_+ \ , \quad \underset{\sim}{y}'' = \underset{\sim}{y} \ , \quad y''_- = \frac{1}{\sqrt{s}}\, y_- \ . \tag{3.8}$$

After these transformations, the exponent appearing in Eq. (3.3) reduces asymptotically to

$$E = -\frac{i}{2}\, e^2 s \int d^4x\, d^4y\ j_+^{(a)}(x')\, D_F(x-y)\, j_-^{(c)}(y'') \ . \tag{3.9}$$

Quantities x'_+ and y''_-, which are of order $0(1/\sqrt{s})$, are Lorentz contracted. So are quantities x_-, y_+ in the c.m. frame.[9] At the infinite s limit, these quantities

are contracted to zero, and may be ignored. Hence

$$E = -\frac{i}{2} e^2 s \int \frac{1}{2\sqrt{s}} dx_+ dx'_- d^2x\, j_+^{(a)}(x'_+ = 0,\ \underset{\sim}{x},\ x'_-)$$

$$\frac{1}{2\sqrt{s}} dy''_+ dy_- d^2y\, j_-^{(c)}(y''_+,\ \underset{\sim}{y},\ y''_- = 0) \qquad (3.10)$$

$$\times D_F(x_+,\ \underset{\sim}{x}-\underset{\sim}{y},\ -y_-) \quad .$$

Carrying out the x_+ and y_- integrals, we have

$$E = -ie^2 \int \frac{1}{2} d^2x\, dx'_-\, j_+^{(a)}(x'_+ = 0,\ \underset{\sim}{x},\ x'_-)$$

$$\frac{1}{2} dy''_+ d^2y\, j_-^{(c)}(y''_+,\ \underset{\sim}{y},\ y''_- = 0)\ \ V(\underset{\sim}{x}-\underset{\sim}{y}) \quad . \qquad (3.11)$$

Since $j_+^{(a)}(x'_+ = 0,\ \underset{\sim}{x},\ x'_-)$'s (and $j_-^{(c)}(y''_+,\ \underset{\sim}{y},\ y''_- = 0)$) commute among themselves, the T-product is the same as an ordinary product. Therefore, we can do the dx'_- and dy''_+ integrals without worrying about the T-product, leading to

$$E = -ie^2 \int d^2x\, d^2y\, \sigma_+(\underset{\sim}{x})\ V(\underset{\sim}{x}-\underset{\sim}{y})\ \sigma_-(\underset{\sim}{y}) \qquad (3.12)$$

with σ_+, σ_- defined in (2.10) and (2.13). Hence, the matrix element (3.3) reduces to

$$\langle A', C'' | \exp\left[-ie^2 \int d^2x\, d^2y\, \sigma_+(\underset{\sim}{x})\ V(\underset{\sim}{x}-\underset{\sim}{y})\ \sigma_-(\underset{\sim}{y})\right] | a', c'' \rangle \qquad (3.13)$$

In terms of the invariant matrix, this is precisely Eq. (2.16).

4. POSSIBLE GENERALIZATION OF THE MODEL

We have shown in previous sections that the operator droplet model may be viewed as the contribution due to a set of Feynman diagrams in Fig. 1. It is natural to ask about possible generalizations of the model if additional sets of diagrams are included.

It is known that diagrams 1 are not the only set of leading diagrams at $s = \infty$. Diagrams with exchange photons interacting among themselves lead to a larger set of diagrams which are also large at $s = \infty$. Some typical diagrams of this larger category are shown in Fig. 2. These diagrams together with possible evaporation diagrams 3 are, we believe, the only diagrams which are large at $s = \infty$.[10] They behave like $s(\ell n s)^N$ at large s where N is the number of primitive bubbles introduced in III. Readers are referred to this reference for details.

Diagrams in Figs. 2 and 3 will no longer give the simple fixed s^1 behavior. Actually, this is important as the fixed s^1 behavior violates unitarity.[11] If we take this larger set of diagrams seriously, we find that the droplet model must be modified. Among other possible modifications (see Section 5), the s-independent potential appearing in the original operator droplet model might be replaced by an s-dependent potential $V(s,\underset{\sim}{x})$. To see how this fits in naturally, we consider diagram (2a). It is shown in III that the over-all amplitude for this type of diagram is

$$\frac{s}{2}\,\frac{\delta_{a'a}}{m}\,\frac{\delta_{c'c}}{m}\int d^2b\; e^{-i\underset{\sim}{k}\cdot\underset{\sim}{b}}\left[e^{i\chi(s,\underset{\sim}{b})} - 1\right] \tag{4.1}$$

with

$$i\chi(s,\underset{\sim}{b}) = \int \frac{d^2k}{(2\pi)^2}\; e^{i\underset{\sim}{k}\cdot\underset{\sim}{b}}\, F(s,\underset{\sim}{k}) \quad , \tag{4.2}$$

$$F(s,\underset{\sim}{k}) = \sum (\text{all connected diagrams with momentum-transfer } \underset{\sim}{k}) \quad . \tag{4.3}$$

A direct calculation from the operator droplet model, in analogy with Lee, gives

$$V(s,\underset{\sim}{x}) = -\chi(s,\underset{\sim}{x}) = \text{Fourier transform of } iF(s,\underset{\sim}{k}) \quad . \tag{4.4}$$

An s-dependent potential obtained by including all connected diagrams should be an important generalization of the original droplet model.

The geometrical meaning of this modification is that the "opaqueness" of the droplet is energy-dependent. Hence, it leads to a slow s-dependence in the forward differential cross section.[12] This is also the physical picture suggested by the Regge model.

Another important class of diagrams that we would like to discuss is that associated with the evaporation of particles from the bubbles. These evaporation particles have a dp_+/p_+ distribution in momentum space, and are qualitatively different from particles emitted from blobs A and C. It is physically sound to identify jet A and jet C emitting from blobs A and C as fragments of the target and the projectile. For evaporation particles, however, there is a uniform distribution in $\ell n\, p_+$ space. The momentum spectrum of these particles spans the entire available range, starting all the way from p_a to p_c. As s increases, the available range of the momentum spectrum increases. Nevertheless, its distribution remains the same (uniform distribution) in $\ell n\, p_+$ space. For this reason, they should not be classified as fragments.[13] The partial amplitude for the evaporation of particles B in Fig. 3b can be computed in an analogous way as

$$(4\pi)^2\, \delta(\Sigma p_+)\, \delta(\Sigma q_-)$$

$$\times \int \Pi\left(\frac{1}{2}\, d^2x\, dx_-\right) \Pi\left(\frac{1}{2}\, dy_+\, d^2y\right) e^{\Sigma i\underset{\sim}{q}\cdot\underset{\sim}{x} - \Sigma i\underset{\sim}{p}\cdot\underset{\sim}{y}}$$

$$\times \langle B|T\left[j_+(x_{1+}=0, \underset{\sim}{x}_1, x_{1-}) \cdots j_-(y_{1+}, \underset{\sim}{y}_1, y_{1-}=0) \cdots\right]|0\rangle \quad (4.5)$$

This result does not reduce simply to products of σ_+ and σ_- because $j_+(x_+=0, \underset{\sim}{x}, x_-)$ and $j_-(y_+, \underset{\sim}{y}, y_-=0)$ do not commute.[14]

5. QUANTUM ELECTRODYNAMICS

The separation of interactions into an interaction without fundamental vector particles and an EM interaction mediated by photon (a vector particle) exchange no longer makes sense in pure quantum electrodynamics (QED). Even though it is still possible to classify a diagram according to its primitive components, as we did in III, summation over diagrams analogous to Fig. 1 does not lead to an expression suggested by the original operator droplet model. This can be understood from the observation that the generalized vertex function

$$\int \Pi dx\, e^{-i\sum q_i \cdot x_i} \langle A|T(j_\mu(x_1)\ldots j_\lambda(x_N))|a\rangle$$

$$\equiv (2\pi)^4\, \delta^4(p_a+q-\sum p_{ai})\, A^{(B.B.)}_{\mu\nu\ldots\lambda}(p_a,q) \qquad (5.1)$$

will give rise to an amplitude which contains all possible N-photon diagrams, including both the primitive and the nonprimitive graphs. This amplitude is denoted by a black box in Fig. 4. Therefore, a partial sum of the graphs, such as Fig. 1, is not sufficient in the present case to generate an expression consistent with an operator droplet model.

The above considerations indicate that a sum over all possible photon exchange diagrams between two black boxes in Fig. 5 should lead to an operator droplet model analogous to the result developed in Sections 2 and 3. Since the black box contains all kinds of nonprimitive graphs, the union of two such black boxes should generate all possible leading graphs, and hence the leading amplitude at $s = \infty$. The amplitude for process $a+c \to A+C$ (i.e., jet A and jet C) obeys relations (2.6) and (2.16) provided that we replace the expressions $\sum A_{++\ldots+}$ and $\sum C_{--\ldots-}$ in (2.6) by the corresponding expressions $A^{(B.B.)}_{++\ldots+}$ and

$C^{(B.B.)}_{--\ldots-}$ for the black boxes. Hence, for N-photon exchange, we have

$$M^{(N)} = \frac{s}{2}\,\frac{1}{N!}\int \Pi\,\frac{dq'_-}{4\pi}\; A^{(B.B.)}_{++\ldots+}(p'_a,q')\; 4\pi\;\delta(\Sigma q'_- - k'_-)$$

$$\Pi\,\frac{dq''_+}{4\pi}\; C^{(B.B.)}_{--\ldots-}(p''_c,q'')\; 4\pi\;\delta(\Sigma q''_+ - k''_+)$$

$$\times\,\Pi\,\frac{d^2q_i}{(2\pi)^2}\,\frac{-ie^2}{q_i^2+\mu^2}\,(2\pi)^2\;\delta^2(\Sigma q_i - k) \quad . \tag{5.2}$$

For the over-all amplitude, we have

$$M(2\pi)^4\;\delta(p'_{a+}-\Sigma p'_{ai+})\;\delta(p''_{c-}-\Sigma p''_{ci-})\;\delta^2(p_a+p_c-\Sigma p_{ai}-\Sigma p_{ci})$$

$$= \frac{s}{2}\left\langle A', C''\middle|\exp\left[-ie^2\int d^2x\, d^2y\;\sigma_+(x)\;V(x-y)\;\sigma_-(y)\right]-1\middle|a', c''\right\rangle \tag{5.3}$$

To make these expressions more precise and hence more useful, we would like to study the black box contribution carefully. Strictly speaking, the perturbation expansion of (5.1), or equivalently the black box expression $A^{(B.B.)}$, does not approach a finite limit at $s = \infty$. (Of course, this does not exclude the possibility that the over-all sum of the perturbation series may converge to a finite limit. However, we shall not investigate this possibility here.) The lowest order (e^6) diagrams which lead to this divergence difficulty are due to the photon-photon interaction, as shown in Fig. 4b. These diagrams are, in fact, the lowest order nonprimitive diagrams. Following the argument given in III, it can be shown that the contribution to Fig. 4b goes like $\ell n\, s_1$ at large s_1, where s_1 is the energy-squared for the incident electron (of momentum p_a) measured in the reference frame. In our language (see paper III, Section 2), $\ell n\, s_1$ is a measure of the available $\ell n\, p_+$ phase space in which the electron loop

can slide freely. If we cut diagram 4b horizontally, we find that the intermediate state consists of an e^+e^- pair. This e^+e^- pair is the simplest evaporation process which we discussed in Section 3. The divergence in (5.1) may be viewed as due to the presence of these virtual evaporation particles in the intermediate state, and reflects the increase of the available phase space as s_1 increases.

Since the subenergy s_1 depends on the particular reference frame, the same arbitrariness will appear in the evaluation of the black box in graph 4. This sounds unpleasant because the physical amplitude should not depend on the particular reference frame being used. However, as we shall see, the dependence on the reference frame is only superficial. This dependence will disappear if graphs related to one another by different partitions are all added together. This is very similar in spirit to the verification of gauge invariance in the usual QED calculations. In general, individual diagrams are not gauge invariant. However, when diagrams with photon vertices permuted in all possible ways on a charged line are included, a gauge invariant result is always obtained.

In the following, we wish to work out a few examples by means of expression (5.2) (or equivalently (5.3)) to reproduce QED perturbation results obtained so far. In particular, we would like to demonstrate how a reference frame independent result emerges and how the correct $(\ell n\, s)^N$ behavior is recovered.

A. Repetition of Bubbles in t-Channel

The first example that we wish to work out is the repetition of bubbles in t-channel, shown in Fig. 6a. The relevant part of the left-hand black box with two external photons are given in Fig. 6b. The partial amplitude for these processes in the black box can be computed by means of the method developed

in III, giving

$$\int \frac{dq'_-}{4\pi} A_{++}^{(B.B.)}(p'_a, q')$$

$$= I_a(q) + \frac{\ln s_1}{4\pi} \int \frac{d^2p}{(2\pi)^2} I_a(p)\, J(p,q)\, \frac{-ie^2}{p_1^2+\mu^2}\, \frac{-ie^2}{p_2^2+\mu^2}$$

$$+ \frac{1}{2!} \left(\frac{\ln s_1}{4\pi}\right)^2 \int \frac{d^2\ell}{(2\pi)^2} \frac{d^2p}{(2\pi)^2} I_a(\ell)\, J(\ell,p)\, J(p,q)\, \frac{-ie^2}{\ell_1^2+\mu^2}\, \frac{-ie^2}{\ell_2^2+\mu^2}\, \frac{-ie^2}{p_1^2+\mu^2}\, \frac{-ie^2}{p_2^2+\mu^2}$$

$$+ \cdots , \qquad (5.4)$$

where I_a and I_c are impact factors for $a \to A$, and $c \to C$, $J(p,q)$ is the loop contribution introduced in III. Similarly, we can compute the right-hand black box

$$\int \frac{dq''_+}{4\pi} C^{(B.B.)}(p''_c, q'')$$

$$= I_c(q) + \frac{\ln s_2}{4\pi} \int \frac{d^2r}{(2\pi)^2} J(q,r)\, I_c(r)\, \frac{-ie^2}{r_1^2+\mu^2}\, \frac{-ie^2}{r_2^2+\mu^2}$$

$$+ \frac{1}{2!} \left(\frac{\ln s_2}{4\pi}\right)^2 \int \frac{d^2r}{(2\pi)^2} \frac{d^2t}{(2\pi)^2} J(q,r)\, J(r,t)\, I_c(t)\, \frac{-ie^2}{r_1^2+\mu^2}\, \frac{-ie^2}{r_2^2+\mu^2}\, \frac{-ie^2}{r_3^2+\mu^2}\, \frac{-ie^2}{r_4^2+\mu^2}$$

$$+ \cdots , \qquad (5.5)$$

where s_2 is the subenergy for particle c in the same reference frame. Simple kinematics tells us that, as $s_{1,2} \to \infty$,[15]

$$\ln s_1 + \ln s_2 \doteq \ln s \quad . \qquad (5.6)$$

In our language, this is simply the additivity of the $\ln p_+$ phase space introduced in III.

The full amplitude is obtained by gluing together the right- and left-hand black boxes through (5.2). The simplest two-photon exchange part without any bubbles gives

$$\frac{s}{2}\,\frac{1}{2!}\quad\frac{d^2q}{(2\pi)^2}\,I_a(\underset{\sim}{q})\,I_c(\underset{\sim}{q})\,\frac{-ie^2}{\underset{\sim}{q}_1^2+\mu^2}\,\frac{-ie^2}{\underset{\sim}{q}_2^2+\mu^2} \tag{5.7}$$

which is trivially correct. Each of the factors in (5.7) is reference frame independent, as is their product.

The first interesting case comes from the single bubble amplitude. It corresponds to the coupling of a one-bubble contribution from one black box to the no-bubble contribution of the other. Diagramatically, it is shown in Fig. 7. The contribution from Fig. 7a,b can be obtained by multiplying the corresponding terms in (5.4) and (5.5), giving

$$\frac{s}{2}\,\frac{1}{2!}\,\frac{\ell n\, s_1}{4\pi}\int\frac{d^2p}{(2\pi)^2}\,\frac{d^2q}{(2\pi)^2}\,I_a(\underset{\sim}{p})\,J(\underset{\sim}{p},\underset{\sim}{q})\,I_c(\underset{\sim}{q})\,\frac{-ie^2}{\underset{\sim}{p}_1^2+\mu^2}\,\frac{-ie^2}{\underset{\sim}{p}_2^2+\mu^2}\,\frac{-ie^2}{\underset{\sim}{q}_1^2+\mu^2}\,\frac{-ie^2}{\underset{\sim}{q}_2^2+\mu^2}\,, \tag{5.8a}$$

and

$$\frac{s}{2}\,\frac{1}{2!}\,\frac{\ell n\, s_2}{4\pi}\int\frac{d^2q}{(2\pi)^2}\,\frac{d^2r}{(2\pi)^2}\,I_a(\underset{\sim}{q})\,J(\underset{\sim}{q},\underset{\sim}{r})\,I_c(\underset{\sim}{r})\,\frac{-ie^2}{\underset{\sim}{q}_1^2+\mu^2}\,\frac{-ie^2}{\underset{\sim}{q}_2^2+\mu^2}\,\frac{-ie^2}{\underset{\sim}{r}_1^2+\mu^2}\,\frac{-ie^2}{\underset{\sim}{r}_2^2+\mu^2}\,, \tag{5.8b}$$

respectively. By adding together these two pieces and making use of (5.6), we obtain

$$\frac{s}{4}\,\frac{\ell n\, s}{4\pi}\int\frac{d^2p}{(2\pi)^2}\,\frac{d^2q}{(2\pi)^2}\,I_a(\underset{\sim}{p})\,J(\underset{\sim}{p},\underset{\sim}{q})\,I_c(\underset{\sim}{q})\,\frac{-ie^2}{\underset{\sim}{p}_1^2+\mu^2}\,\frac{-ie^2}{\underset{\sim}{p}_2^2+\mu^2}\,\frac{-ie^2}{\underset{\sim}{q}_1^2+\mu^2}\,\frac{-ie^2}{\underset{\sim}{q}_2^2+\mu^2}\,. \tag{5.9}$$

Even though each of the individual terms is frame dependent, their sum is not. The final result agrees also with earlier calculations.

To demonstrate that the result holds for multibubble amplitudes, let us work out diagram 8 which involves the repetition of two bubbles. The contribution due to diagrams a, b, and c are

$$\left(\frac{s}{2\cdot 2!}\right)\frac{1}{2!}\left(\frac{\ell n\, s_1}{4\pi}\right)^2 \int \frac{d^2\ell}{(2\pi)^2}\frac{d^2p}{(2\pi)^2}\frac{d^2q}{(2\pi)^2} I_a(\ell)\, J(\ell,p)\, J(p,q)\, I_c(q)$$

$$\times \frac{-ie^2}{\ell_1^2+\mu^2}\frac{-ie^2}{\ell_2^2+\mu^2}\frac{-ie^2}{p_1^2+\mu^2}\frac{-ie^2}{p_2^2+\mu^2}\frac{-ie^2}{q_1^2+\mu^2}\frac{-ie^2}{q_2^2+\mu^2}\ , \qquad (5.10a)$$

$$\left(\frac{s}{2\cdot 2!}\right)\frac{\ell n\, s_1}{4\pi}\frac{\ell n\, s_2}{4\pi} \int \frac{d^2p}{(2\pi)^2}\frac{d^2q}{(2\pi)^2}\frac{d^2r}{(2\pi)^2} I_a(p)\, J(p,q)\, J(q,r)\, I_c(r)$$

$$\times \frac{-ie^2}{p_1^2+\mu^2}\frac{-ie^2}{p_2^2+\mu^2}\frac{-ie^2}{q_1^2+\mu^2}\frac{-ie^2}{q_2^2+\mu^2}\frac{-ie^2}{r_1^2+\mu^2}\frac{-ie^2}{r_2^2+\mu^2}\ , \qquad (5.10b)$$

and

$$\left(\frac{s}{2\cdot 2!}\right)\frac{1}{2!}\left(\frac{\ell n\, s_2}{4\pi}\right)^2 \int \frac{d^2q}{(2\pi)^2}\frac{d^2\ell}{(2\pi)^2}\frac{d^2t}{(2\pi)^2} I_a(q)\, J(q,\ell)\, J(\ell,t)\, I_c(t)$$

$$\times \frac{-ie^2}{q_1^2+\mu^2}\frac{-ie^2}{q_2^2+\mu^2}\frac{-ie^2}{\ell_1^2+\mu^2}\frac{-ie^2}{\ell_2^2+\mu^2}\frac{-ie^2}{t_1^2+\mu^2}\frac{-ie^2}{t_2^2+\mu^2} \qquad (5.10c)$$

respectively. Each of the above expressions contains a frame-dependent factor multiplied by a common frame-independent basic term. Adding all three expressions together, we are led to a frame-independent factor:

$$\frac{1}{2!}\left(\frac{\ell n\, s_1}{4\pi}\right)^2 + \left(\frac{\ell n\, s_1}{4\pi}\right)\left(\frac{\ell n\, s_2}{4\pi}\right) + \frac{1}{2!}\left(\frac{\ell n\, s_2}{4\pi}\right)^2$$

$$= \frac{1}{2!}\left(\frac{\ell n\, s_1 + \ell n\, s_2}{4\pi}\right)^2 = \frac{1}{2!}\left(\frac{\ell n\, s}{4\pi}\right)^2\ , \qquad (5.11)$$

and hence to a final expression

$$\frac{s}{4}\,\frac{1}{2}\left(\frac{\ell n\, s}{4\pi}\right)^2 \int \frac{d^2\ell}{(2\pi)^2}\,\frac{d^2p}{(2\pi)^2}\,\frac{d^2q}{(2\pi)^2}\, I_a(\ell)\, J(\ell,p)\, J(p,q)\, I_c(q)$$

$$\times\ \frac{-ie^2}{\ell_1^2+\mu^2}\,\frac{-ie^2}{\ell_2^2+\mu^2}\,\frac{-ie^2}{p_1^2+\mu^2}\,\frac{-ie^2}{p_2^2+\mu^2}\,\frac{-ie^2}{q_1^2+\mu^2}\,\frac{-ie^2}{q_2^2+\mu^2}\ . \qquad (5.12)$$

Equation (5.12) coincides with our previous calculation. The generalization of the present result to iteration of N-bubbles is straightforward.

B. Iteration of Bubbles in the s-Channel

As a final example, we work out the iteration of two bubbles in s-channel. We shall omit most of the algebra because it is similar to what was used in example A. The diagram that we are dealing with is the e^-e^- scattering amplitude in Fig. 9. The relevant parts in the black box are shown in Fig. 10. This contribution can be worked out as

$$\int \Pi \frac{dq'}{4\pi}\, A^{(B.B.)}(p'_a,q') = \frac{\delta_{a'a}}{m} + \frac{\delta_{a'a}}{m}\left(\frac{\ell n\, s_1}{4\pi}\right)\left[\int \frac{d^2p_1 d^2p_2}{(2\pi)^4}\, J(p_1,p_2;q_1q_2)\right.$$

$$\left.(2\pi)^2\,\delta^2(p_1+p_2-q_{12})\,\frac{-ie^2}{p_1^2+\mu^2}\,\frac{-ie^2}{p_2^2+\mu^2} + \text{perm. of } (1.2,\ 3.4) \text{ in pairs}\right]$$

$$+\ \frac{\delta_{a'a}}{m}\left(\frac{\ell n\, s_1}{4\pi}\right)^2\left[\int \frac{d^2p_1 d^2p_2}{(2\pi)^4}\, J(p_1,p_2;q_1q_2)\,\frac{-ie^2}{(p_1^2+\mu^2)}\,\frac{-ie^2}{(p_2^2+\mu^2)}\,(2\pi)^2\,\delta^2(p_1+p_2-q_{12})\right.$$

$$\times\int \frac{d^2q_{34}}{(2\pi)^4}\, J(p_3,p_4;q_3,q_4)\,\frac{-ie^2}{(p_3^2+\mu^2)}\,\frac{-ie^2}{(p_4^2+\mu^2)}\,(2\pi)^2\,\delta^2(p_3+p_4-q_{34})$$

$$\left.+\ \text{perm. of } (1,2,3,4) \text{ in two pairs}\right] + \ldots \qquad (5.13)$$

with

$$\underset{\sim}{q}_{12} = \underset{\sim}{q}_1 + \underset{\sim}{q}_2 = \underset{\sim}{p}_1 + \underset{\sim}{p}_2 \ , \qquad \underset{\sim}{q}_{34} = \underset{\sim}{q}_3 + \underset{\sim}{q}_4 = \underset{\sim}{p}_3 + \underset{\sim}{p}_4 \ ,$$

where a', a are helicities of the electron before and after the scattering. When one puts the two black boxes together, the various parts which correspond to the processes shown in Fig. 9 give

$$\frac{s}{2}\ \frac{1}{4!}\ \frac{\delta_{a'a}}{m}\ \frac{\delta_{c'c}}{m}\left[3\left(\frac{\ell n\, s_1}{4\pi}\right)^2 + 6\left(\frac{\ell n\, s_1}{4\pi}\right)\left(\frac{\ell n\, s_2}{4\pi}\right) + 3\left(\frac{\ell n\, s_2}{4\pi}\right)^2\right]$$

(a) (b) (c)

$$\times \int \frac{d^2q_1}{(2\pi)^2}\ \frac{d^2q_2}{(2\pi)^2}\ \frac{d^2p_1}{(2\pi)^2}\ \frac{d^2p_2}{(2\pi)^2}\ J(\underset{\sim}{q}_1, \underset{\sim}{q}_2; \underset{\sim}{p}_1, \underset{\sim}{p}_2)\ \frac{-ie^2}{\underset{\sim}{q}_1^2+\mu^2}\ \frac{-ie^2}{\underset{\sim}{q}_2^2+\mu^2}\ \frac{-ie^2}{\underset{\sim}{p}_1^2+\mu^2}\ \frac{-ie^2}{\underset{\sim}{p}_2^2+\mu^2}$$

$$\times \quad (2\pi)^2\, \delta^2(\underset{\sim}{q}_1+\underset{\sim}{q}_2-\underset{\sim}{q}_{12})\ \ (2\pi)^2\, \delta^2(\underset{\sim}{p}_1+\underset{\sim}{p}_2-\underset{\sim}{q}_{12})$$

$$\times \int \frac{d^2q_3}{(2\pi)^2}\ \frac{d^2q_4}{(2\pi)^2}\ \frac{d^2p_3}{(2\pi)^2}\ \frac{d^2p_4}{(2\pi)^2}\ J(\underset{\sim}{q}_3, \underset{\sim}{q}_4; \underset{\sim}{p}_3, \underset{\sim}{p}_4)\ \frac{-ie^2}{\underset{\sim}{q}_3^2+\mu^2}\ \frac{-ie^2}{\underset{\sim}{q}_4^2+\mu^2}\ \frac{-ie^2}{\underset{\sim}{p}_3^2+\mu^2}\ \frac{-ie^2}{\underset{\sim}{p}_4^2+\mu^2}$$

$$\times \quad (2\pi)^2\, \delta^2(\underset{\sim}{q}_3+\underset{\sim}{q}_4-\underset{\sim}{q}_{34})\ (2\pi)^2\, \delta^2(\underset{\sim}{p}_3+\underset{\sim}{p}_4-\underset{\sim}{q}_{34})\ \frac{d^2q_{12}}{(2\pi)^2}\ \frac{d^2q_{34}}{(2\pi)^2}\ (2\pi)^2\, \delta^2(\underset{\sim}{q}_{12}+\underset{\sim}{q}_{34}-\underset{\sim}{k}) \ . \tag{5.14}$$

The factors 3 and 6 come from simple counting. It is easy to see that the $\ell n\, s_1$ and $\ell n\, s_2$ factors combine into 3 $(\ell n\, s/4\pi)^2$, which is frame independent. The two remaining complicated factors are functions of $\underset{\sim}{q}_{12}$ and $\underset{\sim}{q}_{34}$ only, and they are in a convolution form. Hence, the result becomes rather simple in the Fourier space, giving

$$\text{Expression (5.14)} = \frac{s}{2}\ \frac{\delta_{a'a}}{m}\ \frac{\delta_{c'c}}{m} \int d^2b\ e^{i\underset{\sim}{k}\cdot\underset{\sim}{b}}\ \frac{1}{2!}\left[i\chi(\underset{\sim}{s}\cdot\underset{\sim}{b})\right]^2 \ ,$$

where $\chi(s,b)$ is the Fourier transform of

$$\frac{1}{2}\,\frac{\ell n\, s}{4\pi}\int \frac{d^2p_1}{(2\pi)^2}\,\frac{d^2p_2}{(2\pi)^2}\,\frac{d^2q_1}{(2\pi)^2}\,\frac{d^2q_2}{(2\pi)^2}\,J(\underset{\sim}{p},\underset{\sim}{q})\,\frac{-ie^2}{\underset{\sim}{p}_1^2+\mu^2}\,\frac{-ie^2}{\underset{\sim}{p}_2^2+\mu^2}$$

$$\times\,\frac{-ie^2}{\underset{\sim}{q}_1^2+\mu^2}\,\frac{-ie^2}{\underset{\sim}{q}_2^2+\mu^2}\,(2\pi)^2\,\delta^2(\underset{\sim}{p}_1+\underset{\sim}{p}_2-\underset{\sim}{k})\,(2\pi)^2\,\delta^2(\underset{\sim}{q}_1+\underset{\sim}{q}_2-\underset{\sim}{k})$$

This result agrees with the general eikonization obtained in III.

6. COMPARISON AND DISCUSSION

In this paper, we have demonstrated that the asymptotic behavior of QED can be reproduced from an operator droplet model. In particular, we showed that the final expression does not depend on the reference frame. If the asymptotic perturbation of QED indeed leads to a correct description for a general scattering amplitude, one might expect that the operator droplet model could supply a useful framework for the description of hadron physics.

We would like to point out the analogy between our model and the parton picture proposed by Feynman.[6] In a parton model, a fast moving hadron, such as a proton, is described by a group of partons all moving along the direction of the hadron. In general, each of the parton carries a positive fraction x of the total longitudinal momentum. Hadron-hadron scattering can be viewed as the scattering between two groups of partons. Feynman called those partons moving with the first hadron the right movers, and those moving with the second hadron the left movers. For final particles, the left and right movers constitute the "fragments" of target and projectile respectively, as suggested by Benecke, Chou, Yang and Yen.[1]

The physical interesting part of the scattering amplitude is associated with the interactions between partons of "wee" momentum. A "wee" momentum p_w should satisfy the inequalities $p_{a+} \gg p_{w+} \gg p_{c+}$, $p_{a-} \ll p_{w-} \ll p_{c-}$. i.e., a "wee" parton carries a momentum whose plus and minus components are much smaller than the large momentum of the incident hadrons. In our language, a "wee" parton lies somewhere in the middle of the available $\ell n p_+$ phase space. (In a sense, these "wee" partons are analogous to the particles which are associated with bubbles in the middle, such as evaporation particles.) A "wee" parton can not be classified unambiguously into one of the incident hadrons. It is confused as to which particle it belongs to. Its sense of motion, i.e., whether it is a left or right mover, depends critically on the reference frame that we are choosing. A reference frame independent result can only be obtained after "wee" partons moving in both directions are included. This is precisely what we demonstrated in Section 5.

The conclusion obtained in Section 5 is also applicable to a theory with both the strong and EM interactions, as the one studied in Section 3, or to a pure strong interaction theory with the presence of a neutral vector meson. The blackbox defined in Section 3 should now include all kinds of strong and EM processes. One can convince oneself from our lower order calculations that the order by order perturbation result from the operator droplet model reproduces the leading contribution of the amplitude obtained from conventional Feynman diagrams.

One warning should always be kept in mind in summing over these leading diagrams. Although one may show to each finite order of perturbation series that the set of diagrams studied here is leading at $s = \infty$, it is not clear that the sum of all these diagrams should lead to the correct asymptotic amplitude.

It is known that the sum of leading terms sometimes may lead to a completely different result from the exact solution, especially when there is a total cancellation in the leading terms. The golden rule that dominant contributions in any field theory calculations at $s = \infty$ are given by diagrams with pure vector exchange is deduced precisely from a study of the leading diagrams. The rule may fail in an exact theory, especially if the coupling of nonvector interactions are strong.

Finally, we wish to emphasize that the main objective of the present investigation is not to provide a quantitative calculation of the leading $s = \infty$ behavior; but rather, is to extract certain physical pictures from various class of diagrams. The class of diagrams which are responsible for an operator droplet model is pointed out in Sections 3 and 5. The relation between these leading diagrams and the operator droplet model may be more fundamental than the present model calculations imply.

ACKNOWLEDGEMENTS

The author is indebted to Professor Paul Fishbane for many stimulating discussions and a critical reading of the manuscript, to Professor Tung-Mow Yan for helpful discussions in related models. The author wishes to thank Professor Sidney Drell and members of the SLAC theory group for their hospitality during the author's visit at SLAC. Finally, he wishes to express his gratitude to Professor R. Torgerson for many critical comments on the presentation of this paper.

APPENDIX: COMMUTATOR RELATIONS ON THE LIGHT CONE

It was conjectured by Gell-Mann that the equal-time commutator relations between the time components of a vector and another vector (or axial vector) current satisfy an $SU_3 \times SU_3$ current algebra of the form

$$\left[\mathscr{F}^o_a(x), \mathscr{F}^o_b(y)\right] = if_{abc}\, \mathscr{F}^o_c(x)\, \delta^3(\underset{\sim}{x}-\underset{\sim}{y}) \quad \cdots \tag{A.1}$$

where f_{abc} is the structure constant of the SU_3 algebra. We would like to show that, under proper limiting process, Eq. (A.1) implies a similar commutator relations for currents on the light cone $x_+ = y_+$:

$$\left[\frac{1}{2}\, \mathscr{F}_{a+}(x), \frac{1}{2}\, \mathscr{F}_{b+}(y)\right] = if_{abc}\, \frac{1}{2}\, \mathscr{F}_{c+}(x) \times \delta^2(\underset{\sim}{x}-\underset{\sim}{y})\, \delta(x_- - y_-) \tag{A.2}$$

On integration over x_- and y_-, we obtain the operator version of Gell-Mann-Dashen-Fubini sum rule,[16,17]

$$\left[\sigma_{a+}(\underset{\sim}{x}), \sigma_{b+}(\underset{\sim}{y})\right] = if_{abc}\, \sigma_{c+}(\underset{\sim}{x})\, \delta^2(\underset{\sim}{x}-\underset{\sim}{y}) \quad . \tag{A.3}$$

To obtain (A.2) from (A.1), we make a Lorentz transformation along the third axis,

$$U\, j^o(x)\, U^{-1} = \cosh\lambda\, j^o(x') + \sinh\lambda\, j^3(x')$$

$$= \frac{1}{2}\, e^{\lambda}\, j_+(x') + \frac{1}{2}\, e^{-\lambda}\, j_-(x')$$

with

$$x'_+ = e^{-\lambda} x^3, \qquad (x^o = 0)$$

$$\underset{\sim}{x}'_\perp = \underset{\sim}{x}_\perp\ , \qquad x'_- = -\, e^{\lambda} x^3 \quad .$$

For fixed x'_- and $e^\lambda \to \infty$, we have

$$\left[\frac{1}{2}\, e^\lambda\, j_+(x'_+=0, \underset{\sim}{x}, x'_-),\qquad \frac{1}{2}\, e^\lambda\, j_+(y_+=0, \underset{\sim}{y}, y'_-)\right]$$

$$= \frac{1}{2}\, e^\lambda\, j_+(0, \underset{\sim}{x}, x'_-)\; \delta^2(\underset{\sim}{x}-\underset{\sim}{y})\;\; \varepsilon\left[e^{-\lambda}(x'_- - y'_-)\right]$$

Cancelling out factors e^λ, we get (A.2).

As a justification of the limiting procedure, the validity of Eq. (A.2) can be checked independently from various free particle models. With the help of the equations of motion, Eq. (A.2) is found to be satisfied for both scalar and Dirac fields.

In the simple case of QED, we know that charge density operators, $j^0(x)$'s, commute among themselves at equal time. Hence, $j_+(x)$'s commute among themselves on the light cone $x_+ =$ constant. The last relation is precisely what we need to prove Eq. (2.9).

REFERENCES AND FOOTNOTES

1. T. T. Chou and C. N. Yang, Phys. Rev. 170, 1591 (1968); 175, 1832 (1968); J. Benecke, T. T. Chou, C. N. Yang and E. Yen, Phys. Rev. 188, 2159 (1969).
2. B. Lee, Phys. Rev. D.1, 2361 (1970).
3. H. Cheng and T. T. Wu, Phys. Rev. Letters 22, 666 (1969); Phys. Rev. 182, 1852; 1868; 1873; 1899 (1969), and to be published.
4. S. J. Chang and S. Ma, Phys. Rev. 180, 1506; 188, 2385 (1969); thereafter referred as I and II; S. J. Chang and P. M. Fishbane, "Scattering amplitudes in quantum electrodynamics at infinite energy and possible implications for hadron physics," Phys. Rev. (to be published), thereafter referred as III.
5. See Section 3 in III.
6. R. P. Feynman in Third International Conference on High Energy Collisions held at SUNY, Stony Brook, New York, Sept. 1969 (Gordon and Breach, Science Publishers, Inc., New York, 1969).
7. J. D. Bjorken, "Theoretical ideas on high-energy inelastic electron-proton scattering," Invited paper at the APS New York meeting (February 1969); J. D. Bjorken and E. A. Paschos, Phys. Rev. 185, 1975 (1969).
8. The one-particle states are normalized covariantly. $\langle p'|p\rangle = (2\pi)^3\, 2E\, \delta^3(p'-p)$ for bosons and $(2\pi)^3\, (E/m)\, \delta^3(p'-p)$ for fermions.
9. What is important here is that we can always ignore x_- in comparison with y_-, and y_+ in comparison with x_+. The relative magnitude of x_-, y_+ vs y_-, x_+ is independent of the particular reference frame (here the c.m. frame) that we are using.
10. These are the diagrams which have the following nice properties: (1) The infinite momenta p_{a+} and p_{c-} have separate pathways. (2) The two infinite

parts are linked by photons only. See II for detailed discussion. Note that even though these diagrams give rise to leading contribution to each order of perturbation theory, it is not clear that the sum of all these diagrams is still leading. A recent calculation (S. J. Chang and T. M. Yan, to be published) indicates that diagrams with scalar meson (or Dirac particle) exchange can give rise to an amplitude comparable in magnitude to those obtained from pure vector exchange.

11. V. N. Gribov and I. Ya Pomeranchuk, Phys. Letters 2, 239 (1962).

12. Recent experiments on p-p scattering seem to support such a slow s-dependence. See G. G. Beznogikh et al., Phys. Rev. Letters 30B, 274 (1969).

13. The particles emitted from a single bubble are kinematically related. Whether these particles are responsible for a "pionization" effect will certainly depend on how one interprets the data.

14. By identifying T as x_+ (or x_-) - ordering, we can move all j_+ (or j_-) together and reduce them to σ_+ (or σ_-). However, one can not do this simultaneously for both j_+ and j_-.

15. This relation can be obtained as follows: Let p'_a, p_a and p''_a be the momenta of particle a in the target, the reference, and the projectile frames; then $\ell n\, s_1 \doteqdot \ell n\, p'_{a+} - \ell n\, p_{a+}$, $\ell n\, s_2 \doteqdot \ell n\, p_{a+} - \ell n\, p''_{a+}$, and $\ell n\, s \doteqdot \ell n\, p'_{a+} - \ell n\, p''_{a+}$. The relation $\ell n\, s_1 + \ell n\, s_2 = \ell n\, s$ then follows. This type of relation is well-known in multiperipheral processes.

16. R. Dashen and M. Gell-Mann, Phys. Rev. Letters 17, 340 (1966); S. Fubini and G. Furlan, Phys. 1, 229 (1964).

17. K. Bardakci and M. B. Halpern, Phys. Rev. 176, 1686 (1968).

FIGURE CAPTIONS

1. A pure multiphoton-exchange diagram without further photon-photon interactions. In Sections 2 and 3, the blobs contain only the strong interactions.
2. Multiphoton-exchange diagrams with further photon-photon interactions. (a) A typical diagram without any vertex corrections on the incident fermion lines. (b) A general diagram with two bubbles.
3. (a) A diagram analogous to 2a but with evaporation particles from one bubble. (b) The evaporation bubble in more detail.
4. (a) The diagramatic expansion of a typical black box. (b) The lowest order processes which contribute to the logarithmic divergence of the black box.
5. The union of two black box diagrams. This symbolic diagram contains all leading Feynman diagrams in QED.
6. (a) A diagram with repetition of bubbles in t-channel. (b) The relevant partial amplitudes in a black-box expansion.
7. Diagrams (a) and (b) are special cases of Fig. 5. The subgraphs on one side of the dotted line belong to a black box. Similarly, the subgraphs on the other side of the line belong to a different black box. The sum of (a), (b) gives rise to a reference-frame-independent result.
8. Same as Fig. 7 with two linked bubbles.
9. Same as Fig. 7 with two bubbles iterated in s-channel.
10. Relevant partial amplitudes in a black-box expansion for the processes given in Fig. 9.

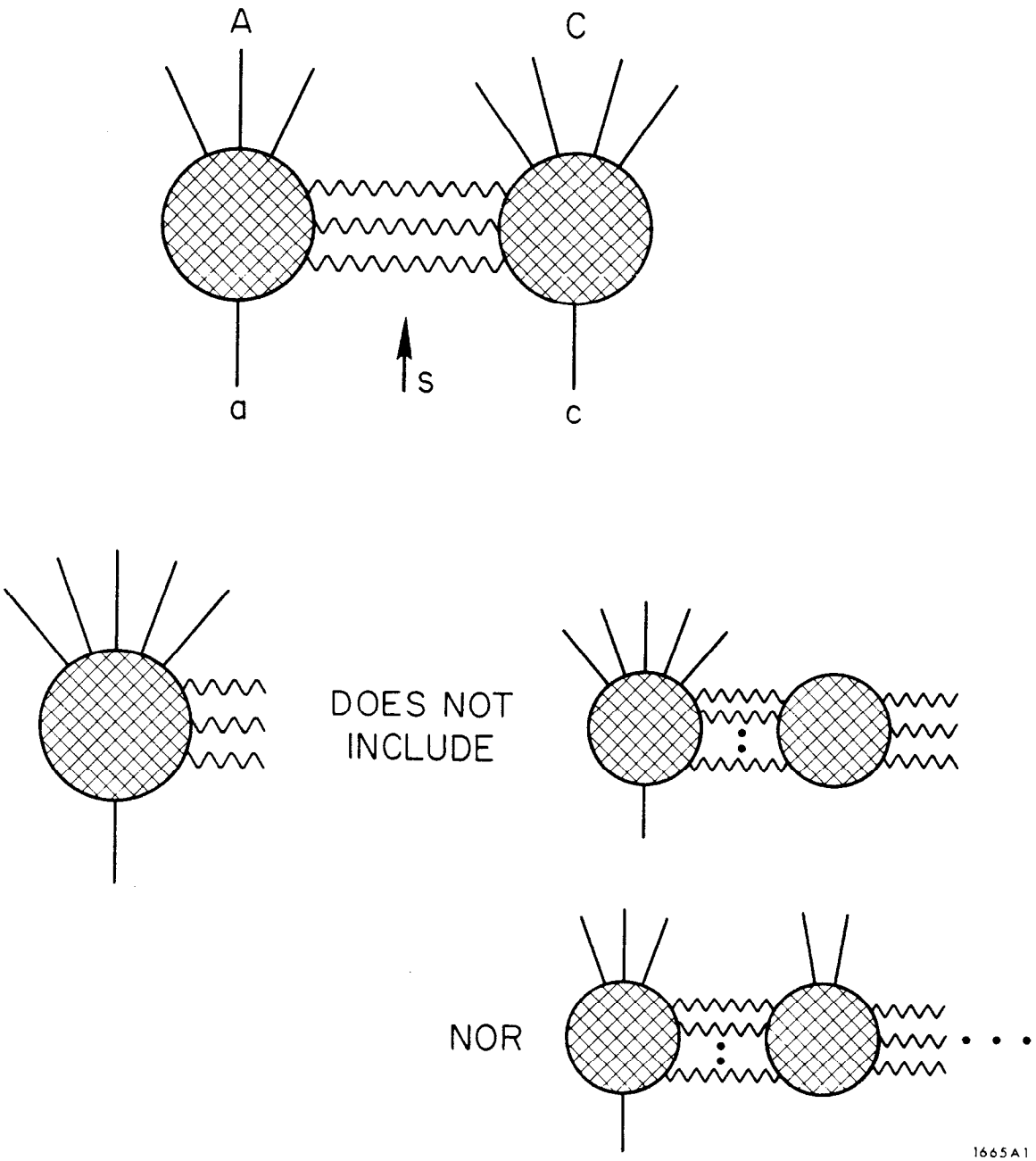

Fig. 1

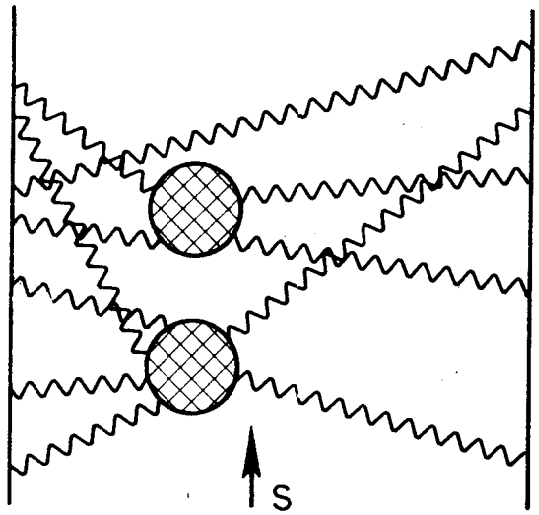

(a)

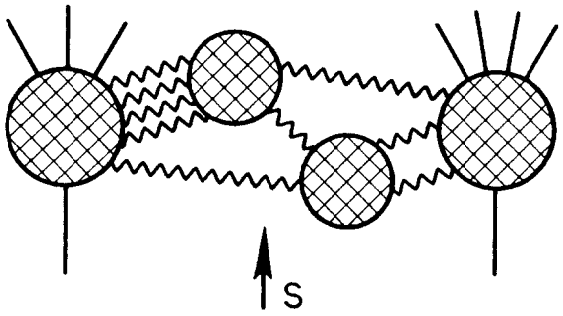

(b)

1665A2

Fig. 2

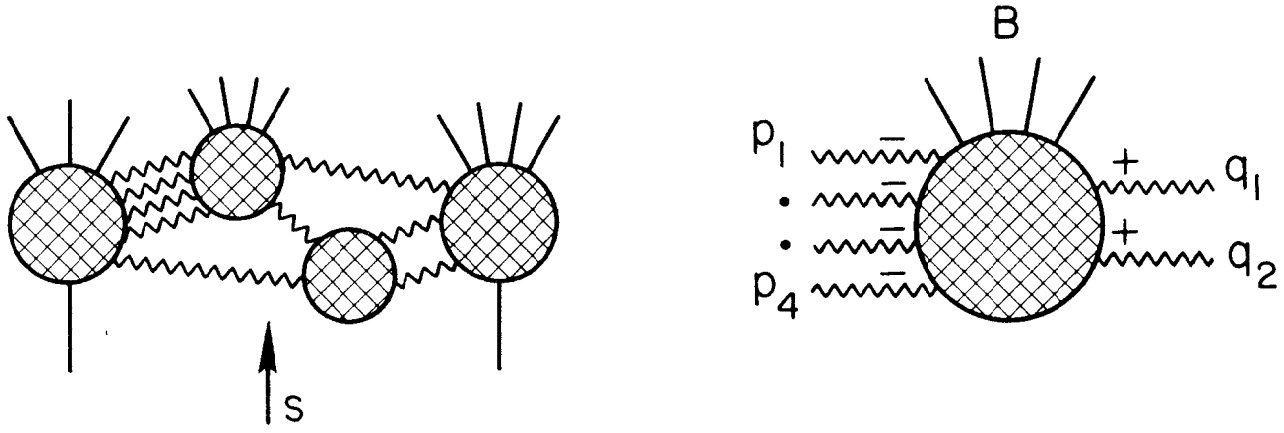

Fig. 3

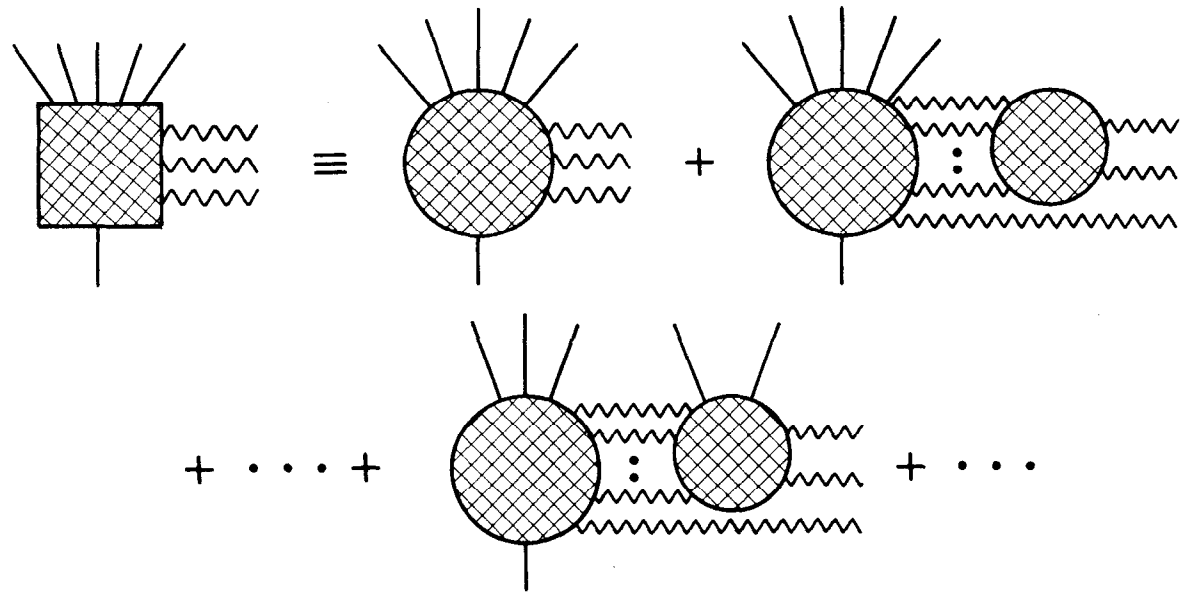

(a)

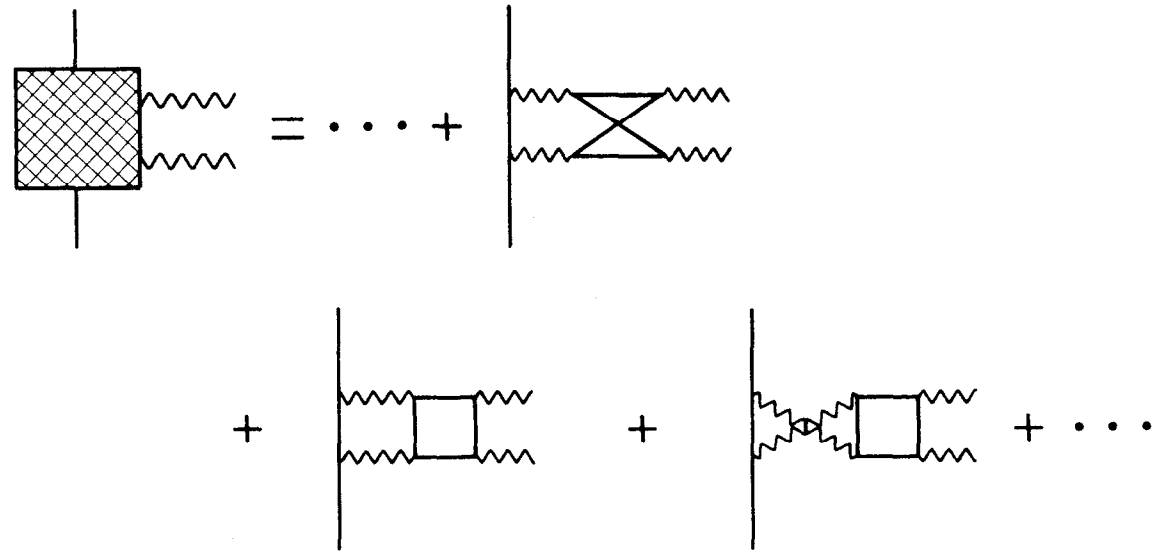

(b)

1665A4

Fig. 4

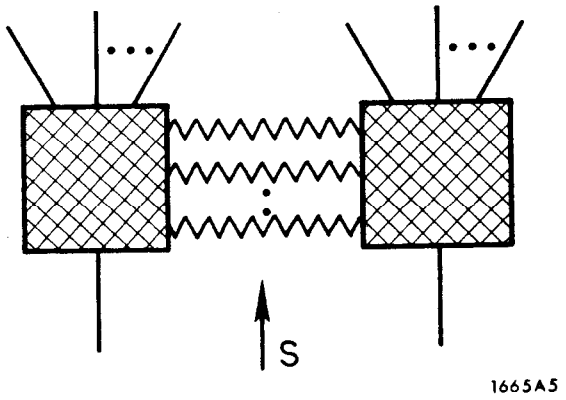

Fig. 5

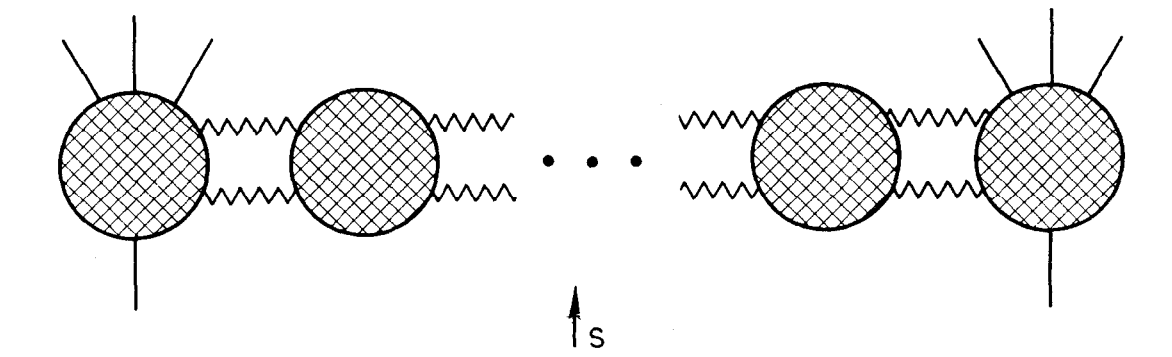

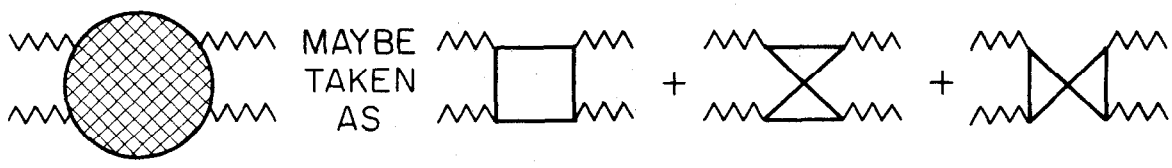

(a)

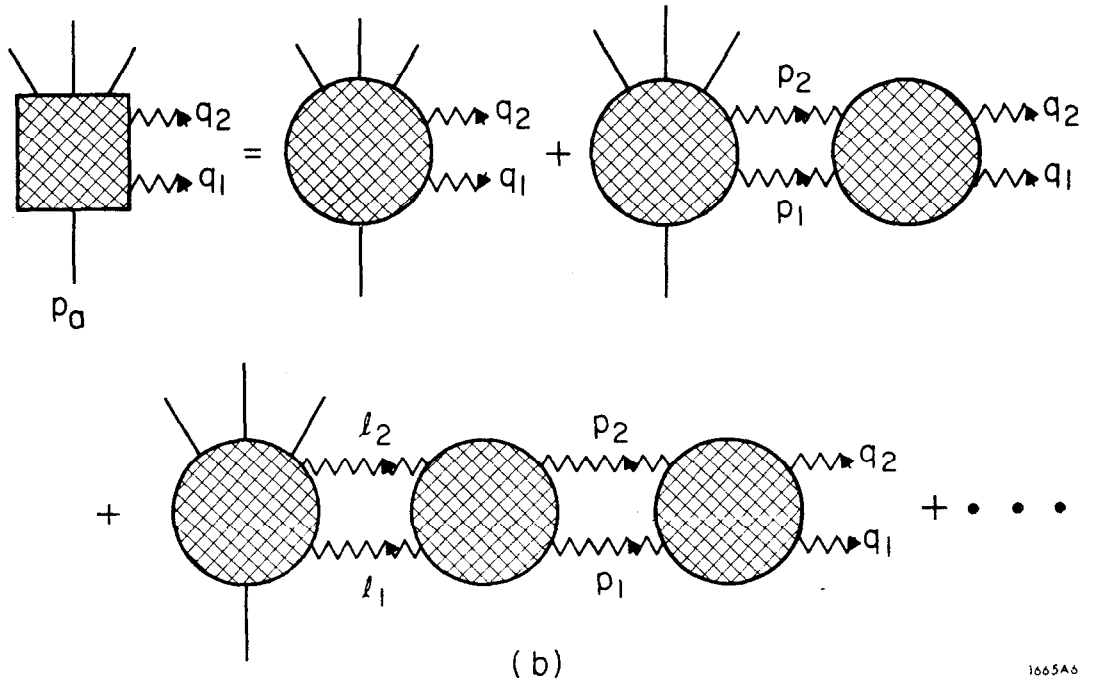

(b)

1665A6

Fig. 6

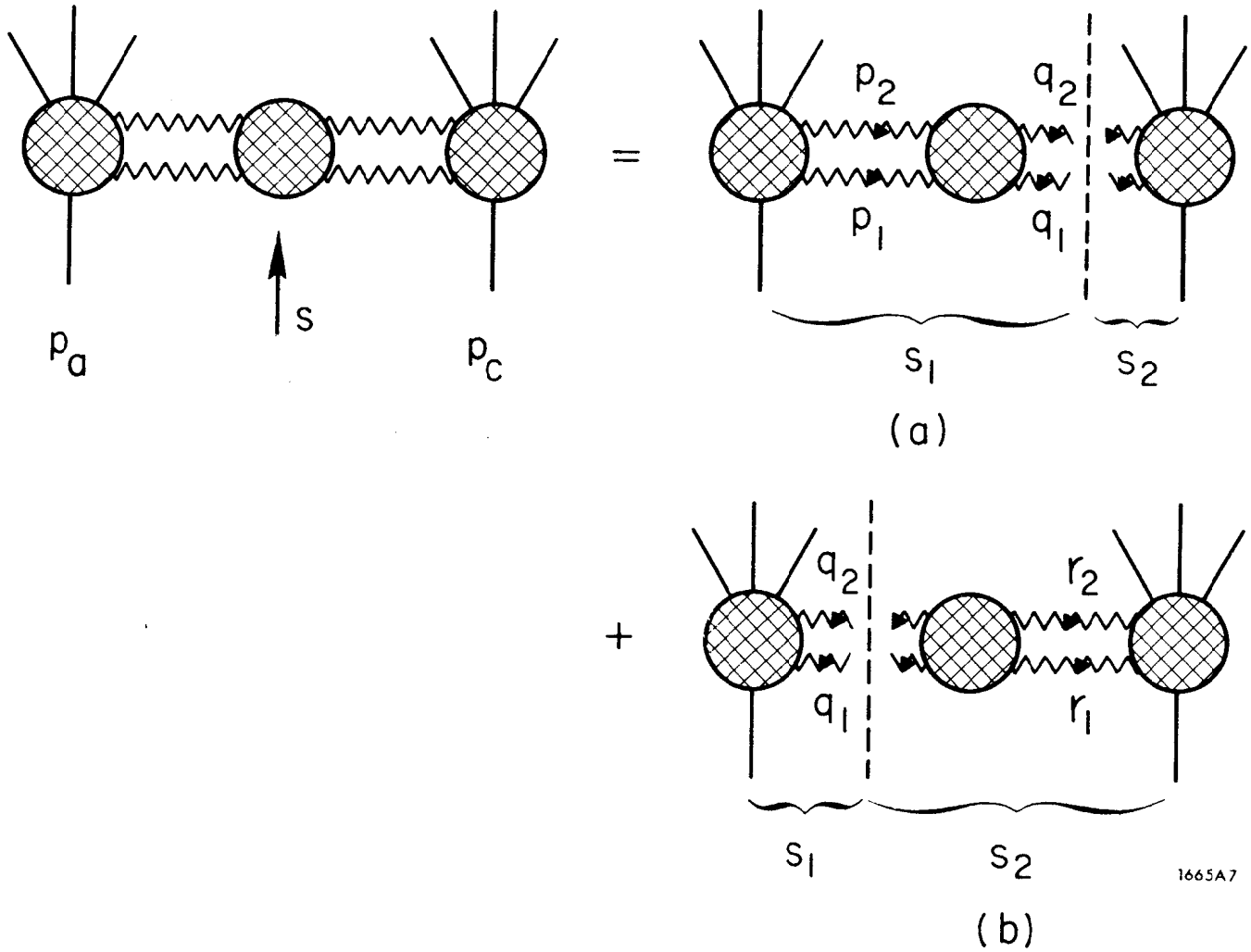

Fig. 7

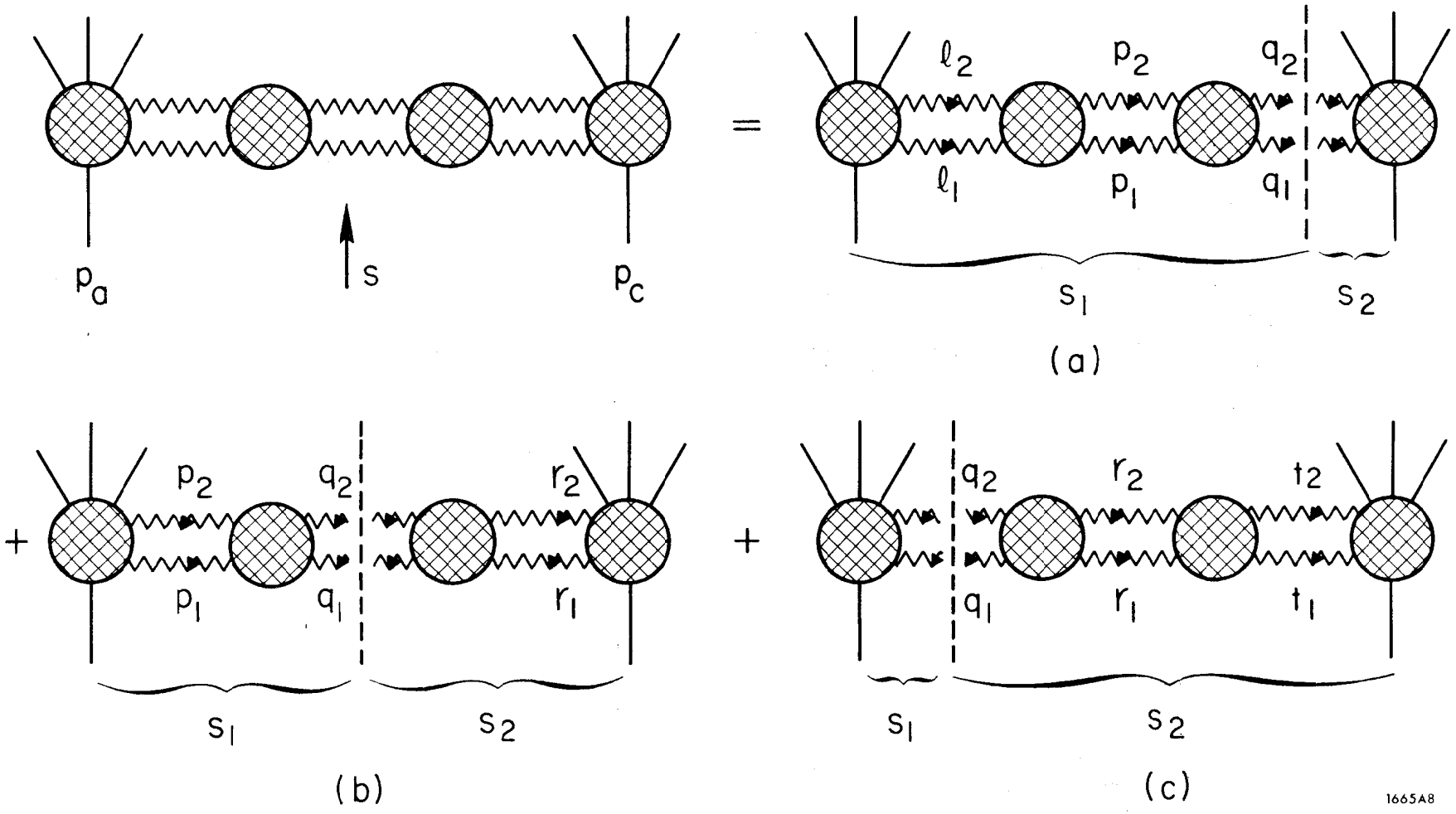
p_a
s
p_c
=
ℓ_2
p_2
q_2
ℓ_1
p_1
q_1
s_1
s_2
(a)
+
p_2
q_2
r_2
p_1
q_1
r_1
s_1
s_2
(b)
+
q_2
r_2
t_2
q_1
r_1
t_1
s_1
s_2
(c)
1665A8

Fig. 8

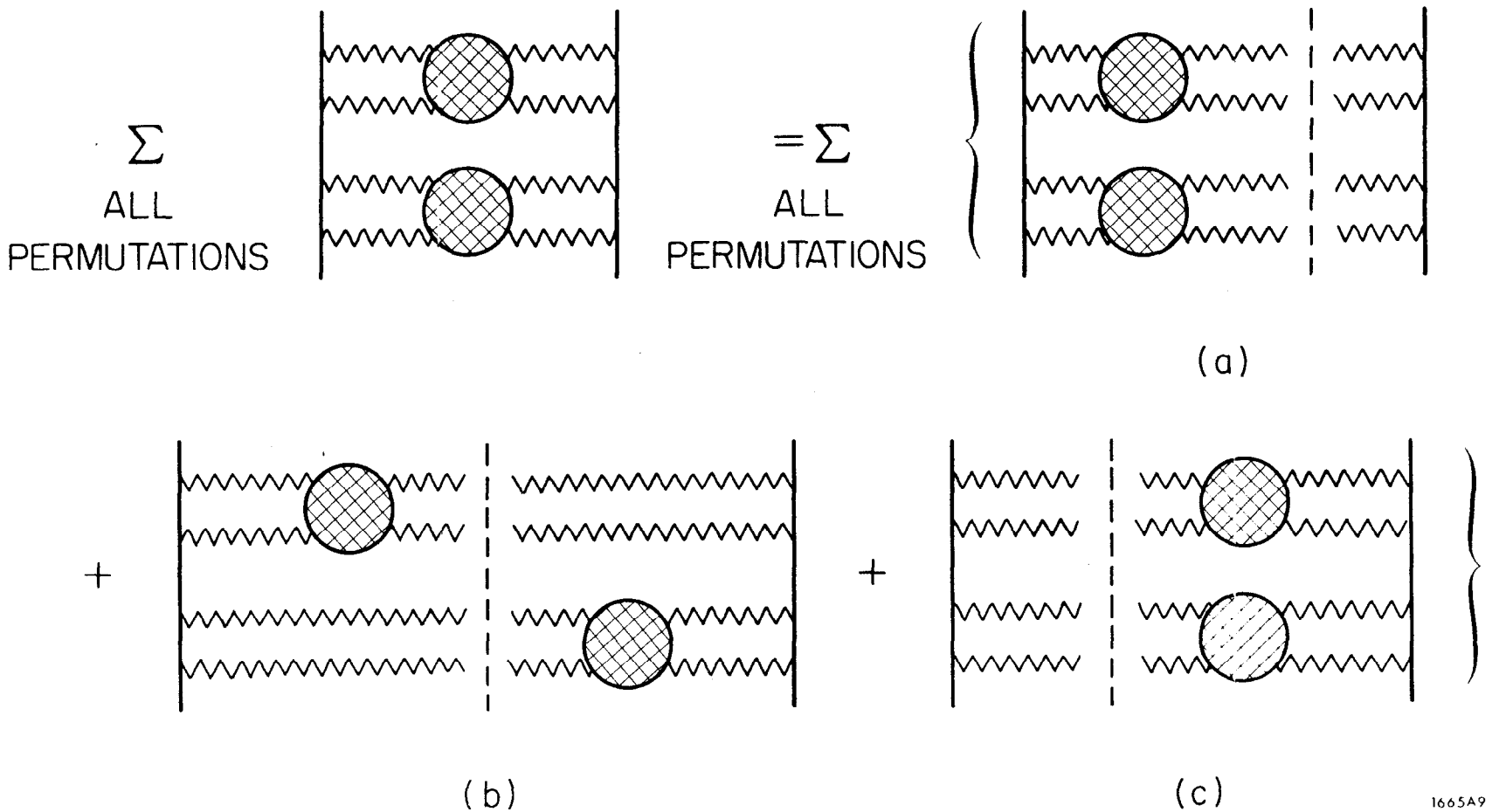

Fig. 9

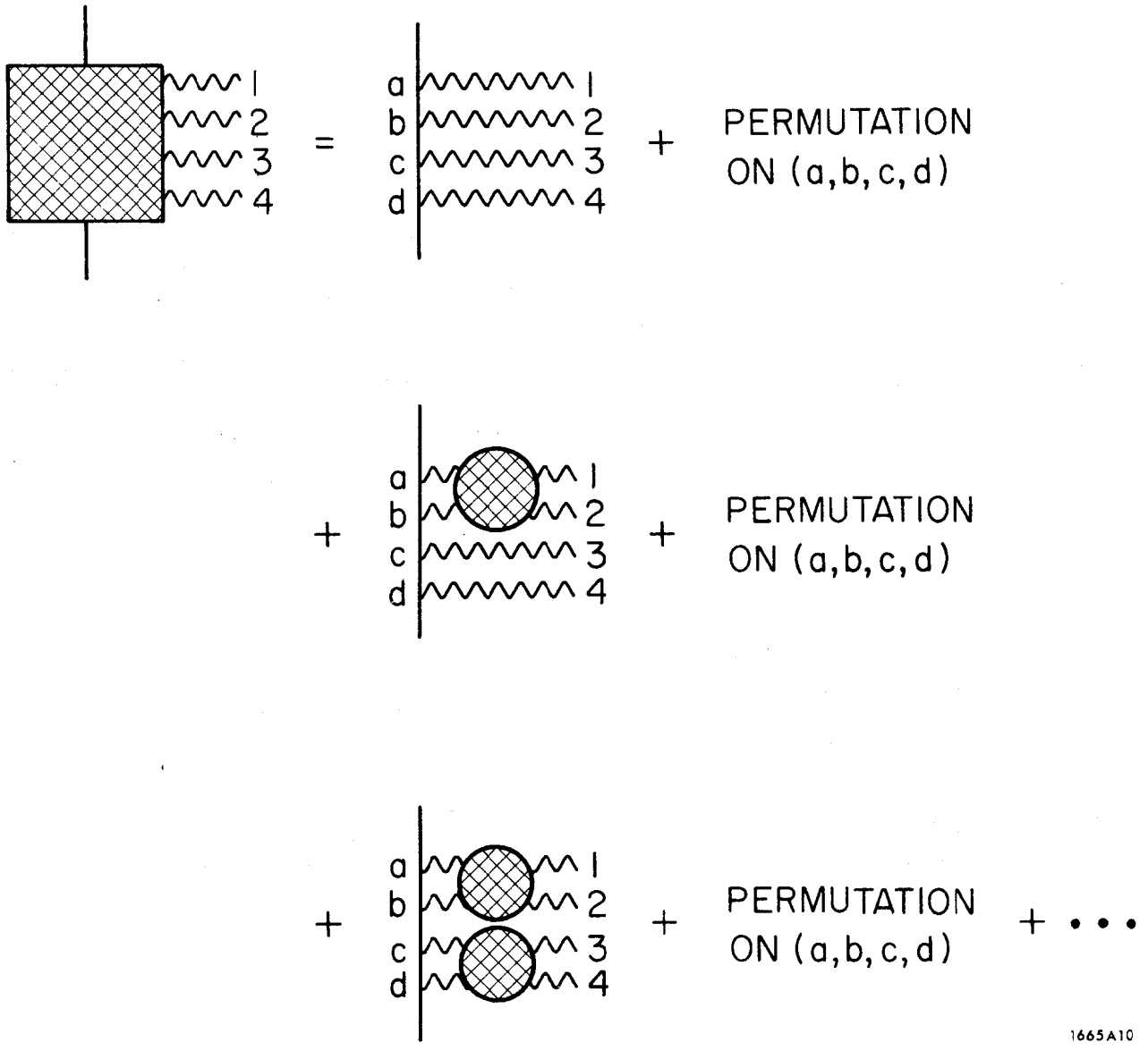
1
2
3
4
=
a
b
c
d
1
2
3
4
+
PERMUTATION
ON (a,b,c,d)
+
a
b
c
d
1
2
3
4
+
PERMUTATION
ON (a,b,c,d)
+
a
b
c
d
1
2
3
4
+
PERMUTATION
ON (a,b,c,d)
+ • • •
1665A10

Fig. 10